British Journal of Pharmacology (2008) 153, 1528–1537
 0007–1188/08 $30.00
www.brjpharmacol.org

RESEARCH PAPER

Thrombin-promoted release of UDP-glucose from human astrocytoma cells

SM Kreda, L Seminario-Vidal, C van Heusden and ER Lazarowski

Cystic Fibrosis/Pulmonary Research and Treatment Center, University of North Carolina School of Medicine, Chapel Hill, NC, USA

Background and purpose: The $P2Y_{14}$ receptor is activated by UDP-sugars, most potently by UDP-glucose, but not by free nucleotides, suggesting that UDP-glucose is the cognate agonist for this receptor. However, evidence for regulated release of UDP-glucose is scarce. In the present study, the occurrence of receptor-promoted release of UDP-glucose was investigated, using 1321N1 human astrocytoma cells.
Experimental approach: UDP-glucose release and hydrolysis were measured using HPLC-based techniques. Phospholipase C activation and actin cytoskeleton reorganization were assessed by measuring inositol phosphate formation and fluorescence confocal microscopy, respectively.
Key results: Thrombin and the protease-activating receptor-1 (PAR1) peptide TFLLRNPNDK (PAR1-AP) evoked the release of UDP-glucose and ATP, which was accompanied by enhanced inositol phosphate formation. Although carbachol promoted fourfold greater inositol phosphate formation than thrombin, it failed to promote nucleotide release. Thrombin-promoted nucleotide release was inhibited by BAPTA-AM, brefeldin A and cytochalasin D, and was insensitive to Pertussis toxin and PI3-kinase inhibitors. Thrombin, but not carbachol, induced actin cytoskeleton reorganization, a hallmark of Rho activation in 1321N1 cells. However, PAR-promoted UDP-glucose release was not affected by Rho kinase inhibition.
Conclusions and implications: PAR1-evoked UDP-glucose release reflected a Ca^{2+}-dependent mechanism, engaging additional signalling independently of G_i and Rho kinase activation and requiring a functional actin cytoskeleton and Golgi structures. Our study demonstrates the occurrence of Ca^{2+}-dependent release of UDP-glucose from astrocytoma cells in response to a physiologically relevant stimulus, that is, a G-protein-coupled receptor agonist. Given the presence of $P2Y_{14}$ receptors in astrocytes, UDP-glucose may have important autocrine/paracrine functions in the brain.
British Journal of Pharmacology (2008) **153**, 1528–1537; doi:10.1038/sj.bjp.0707692; published online 21 January 2008

Keywords: PAR1; thrombin; nucleotide release; UDP-glucose; 1321N1 human astrocytoma cells; $P2Y_{14}$ receptor

Abbreviations: β,γ-metATP, β,γ-methylene ATP; BFA, brefeldin A; DAPI, 4,6-diamidino-2-phenylindole; E-NPP, ecto-nucleotide pyrophosphatase; PAR, protease-activated receptor; PAR1-AP, PAR1-activating peptide; ROCK, Rho kinase

Introduction

ATP and other nucleotides are released from cells in a regulated manner to accomplish extracellular signalling functions through activation of P2X and P2Y purinergic receptors (Burnstock and Williams, 2000; Burnstock, 2006). P2X receptors, comprising seven species ($P2X_1$–$P2X_7$), are ATP-gated ion channels. P2Y receptors belong to the superfamily of G-protein-coupled receptors. At least eight P2Y receptor species have been identified, seven of which are activated by adenine and/or uridine nucleoside di- and triphosphates. The $P2Y_1$, $P2Y_{12}$ and $P2Y_{13}$ receptors are activated by ADP. The $P2Y_2$ receptor is activated by both ATP and UTP, and the $P2Y_4$ (human) and $P2Y_6$ receptors are activated by UTP and UDP, respectively. Unlike other P2 receptors, the $P2Y_{14}$ receptor is activated by UDP-sugars, most potently by UDP-glucose, and is not activated by di- or triphosphonucleotides (Chambers *et al.*, 2000).

Studies using heterologously expressed $P2Y_{14}$ receptor have revealed a previously unnoticed accumulation of endogenous receptor agonist in extracellular solutions. Taking advantage of the selectivity of UDP-glucose pyrophophorylase in catalyzing the UDP-glucose-dependent conversion of pyrophosphate to UTP, UDP-glucose was identified and quantified with nanomolar sensitivity in the extracellular medium of many tissues and cell lines, including 1321N1 human astrocytoma cells (Lazarowski *et al.*, 2003b). However, whether extracellular accumulation of UDP-glucose reflects a regulated mechanism of nucleotide release

Correspondence: Dr ER Lazarowski, Cystic Fibrosis/Pulmonary Research and Treatment Center, University of North Carolina School of Medicine, 7017 Thurston-Bowles Building, CB 7248, Chapel Hill, NC 27599-7248, USA.
E-mail: Eduardo_Lazarowski@med.unc.edu
Received 21 September 2007; revised 3 December 2007; accepted 12 December 2007; published online 21 January 2008

is not well defined. With the exception of nerve terminals and other specialized tissues that release ATP from secretory granules through Ca^{2+}-regulated exocytosis, how nucleotides are released from most cell types is poorly understood. A major limitation in this understanding was, until recently, the paucity of pharmacological tools to induce nucleotide release in a regulated manner.

Thrombin and other serine proteases activate a family of four G-protein-coupled receptors, referred to as protease-activated receptors (PAR1–PAR4). Recently, Joseph *et al.* (2003) illustrated that activation of 1321N1 cells with thrombin resulted in enhanced release of ATP in a Ca^{2+}-dependent manner. Subsequently, we observed that addition of thrombin to 1321N1 cells resulted in enhanced extracellular accumulation of UDP-glucose, in addition to ATP release (Lazarowski, 2006). However, whether thrombin-increased UDP-glucose accumulation reflected PAR-promoted UDP-sugar release and whether the signalling pathways were potentially involved in such a release were not addressed. In the present study, we investigated potential mechanisms involved in thrombin-elicited UDP-glucose release in 1321N1 cells. As the $P2Y_{14}$ receptor is abundantly expressed in brain astrocytes (Moore *et al.*, 2003), illustration of the regulated release of UDP-glucose by 1321N1 astrocytoma cells would provide support for the physiological significance of the $P2Y_{14}$ receptor in the brain.

Methods

Cell culture

1321N1 Human astrocytoma cells were grown in 5% calf serum-supplemented Dulbecco's modified Eagle's medium for 5 days to near confluence (~ 5 to 8×10^5 cells cm^{-2}) on either 35 mm (9.6 cm^2) plastic dishes for real-time ATP measurements or 24-well plastic plates (1.8 cm^2) for UDP-glucose and inositol phosphate measurements, as described previously (Lazarowski *et al.*, 2003b). For confocal microscopy studies, cells were grown to subconfluence on eight-well Lab-Tek II glass chamber slides (Nalge Nunc Int., Naperville, IL, USA). Cells were used within passages 3–12; a gradual decline in PAR1-promoted second messenger production was noted during subsequent passages.

UDP-glucose release

Cultures were rinsed and preincubated in serum-free minimum essential medium for 2 h to allow recovery from mechanical stress during medium changes (Lazarowski *et al.*, 2003b). Incubations were initiated by the addition of drugs, and aliquots (200 μl) were removed at the indicated times. Collected samples were heated (95 °C, 2 min) to inactivate potentially secreted nucleotidases, and stored at −20 °C for nucleotide analysis. UDP-glucose was assayed based on the UDP-glucose pyrophosphorylase-catalyzed conversion of [^{32}P]pyrophosphate to [^{32}P]UTP, followed by HPLC analysis of the resulting [^{32}P]species, as described previously (Lazarowski *et al.*, 2003b).

Measurement of UDP-[^{3}H]glucose metabolism

Cells were rinsed and preincubated as above, and subsequently incubated for the indicated times in 0.3 ml minimum essential medium in the presence of 0.1 μCi UDP-[^{3}H]glucose. The resulting species were analyzed by HPLC as described previously (Lazarowski *et al.*, 2003b).

ATP release

ATP measurements were performed in real time, as described recently (Okada *et al.*, 2006). Briefly, 1321N1 cells were rinsed twice with Hanks' balanced salt solution supplemented with 1.2 mM $CaCl_2$, 1.2 mM $MgCl_2$ and 25 mM HEPES (pH 7.4). Cultures were preincubated for 1 h at 37 °C in 1 ml Hanks' balanced salt solution and transferred to a Turner TD-20/20 luminometer (Turner Biosystems, Sunnyvale, CA, USA). Luciferase (4 μg ml^{-1}; 15 to 30×10^6 light units mg^{-1}) and luciferin (60 μM) were added, and luminescence measured every 30 s. To minimize ATP hydrolysis, the nucleotidase inhibitor β,γ-methylene ATP (β,γ-metATP; 300 μM) was added to the cells 5–10 min before the administration of drugs. Calibration curves using known concentrations of ATP were calculated at the end of each assay.

Inositol phosphate accumulation

The cells were incubated overnight in 0.5 ml of inositol-free HEPES-buffered Dulbecco's modified Eagle's medium (pH 7.4) containing 0.5 μCi of *myo*-[^{3}H]inositol. At the end of the labelling period, cells were preincubated for 10 min in the presence of 10 mM LiCl, followed by the addition of either vehicle or agonist. [^{3}H]Inositol phosphates were isolated on Dowex anion exchange columns and quantified as described previously (Lazarowski *et al.*, 2003b).

Reverse transcription-PCR analysis of PARs

Total RNA was prepared from 1321N1 cells using the RNeasy mini kit (Qiagen Inc., Valencia, CA, USA) after RNAlater treatment (Ambion, Austin, TX, USA). Genomic DNA contamination was removed by DNase treatment and RNA was reverse-transcribed using SuperScript II reverse transcriptase. The resulting cDNA was used as a template, and PCR was performed at the University of North Carolina CF Center Molecular Biology Core Lab (Chapel Hill, NC, USA) according to the following protocol: 4 min at 94 °C, 1 min at 72 °C, 45 s at 94 °C, 1 min at 55 °C and 1 min at 72 °C for 36 cycles, followed by an 8-min incubation at 72 °C. PAR1 (GenBank M62424) primers, kindly provided by Dr JoAnn Trejo (Department of Pharmacology, UNC, NC, USA), were as follows: forward primer, CAGTTTGGGTCTGAATTGTGTCG; reverse primer, TGCACGAGCTTATGCTGCTGAC. Amplified products (predicted size, 591 bp) were sequenced at the UNC Genome Analysis Facility.

Confocal microscopy studies

Cells were incubated with agonists and/or inhibitors, as indicated in the figure legends. At the end of the incubation, cells were fixed in 4% paraformaldehyde at 37 °C for 5 min,

rinsed and permeabilized with 100% cold methanol for 2 min. The actin cytoskeleton was labelled with Alexa 488-phalloidin (70 nM, 60 min at room temperature; Molecular Probes, Eugene, OR, USA). The Golgi was stained with *N*-(4,4-difluoro-5,7-dimethyl-4-bora-3a,4a-diaza-s-indacene-3-pentanoyl)sphingosine (NBD C_6-ceramide; 1 μM, 30 min at 4 °C; Molecular Probes). Cell preparations were mounted under a coverslip with Vectashield medium containing 4,6-diamidino-2-phenylindole (DAPI) (Vector Labs Inc., Burlingame, CA, USA). Confocal microscopy analysis was performed in a Leica SP2 AOBS system, using a ×63 PlanApo lens and two independent laser sources (351 nm UV and 488 nm argon); parameters were saved in a file and used throughout the analyses.

Data analysis

UDP-glucose decay data and agonist concentration–effect relationships were analysed using SigmaPlot 8.01 (SPSS Inc., Chicago, IL, USA). Differences between means were determined by Student's *t*-test and were considered significant when $P<0.01$.

Reagents

[γ^{32}P]ATP (3000 Ci mmol^{-1}) and *myo*-[^{3}H]inositol (20 Ci mmol^{-1}) were purchased from Amersham Pharmacia Biotech (Piscataway, NJ, USA). UDP-glucose pyrophosphorylase from baker's yeast and β,γ-metATP were obtained from Sigma (St Louis, MO, USA). Human α-thrombin was purchased from Enzyme Research Laboratories (South Bend, IN, USA). The PAR1-activating peptide TFLLRNPNDK (Damiano *et al*., 1999), hereafter referred to as PAR1-AP, was synthesized at Tufts University Peptide Synthesis Core Facility (Sommerville, MA, USA). Alexa 488-phalloidin and the fluorescent Golgi marker NBD C_6-ceramide were purchased from Molecular Probes. Rho-associated kinase (Rho-kinase, ROCK) inhibitors Y27632 and H-1152P were purchased from Calbiochem (La Jolla, CA, USA). Other chemicals, of the highest purity available, were obtained from sources previously reported (Lazarowski *et al*., 2003b, 2004).

Results

Stability of extracellular UDP-glucose

Studies of nucleotide release have been complicated by the presence of nucleotidase activities flanking the nucleotide release site (Joseph *et al*., 2003). In addition, nucleoside diphosphokinase and adenylate kinase transfer the terminal phosphate of NTP to NDP or NMP, respectively, creating additional artifacts. Although free nucleotides (that is, NTPs and NDPs) are substrates for most of these activities, UDP-sugars are not metabolized by ecto-apyrases (NTPDases), nucleoside diphosphokinase or adenylate kinase. However, ecto-NTP pyrophosphatases (E-NPP), which hydrolyze free nucleotides as well as cyclic nucleotides, dinucleotides and nucleotide-sugars, are expressed on many cell types, including 1321N1 cells (Lazarowski *et al*., 2000; Joseph *et al*., 2004). Indeed, we have previously illustrated that radiolabelled UDP-glucose was steadily, although relatively slowly, hydrolyzed on 1321N1 cells (Lazarowski *et al*., 2003b).

To optimize conditions that would minimize UDP-glucose metabolism during measurements of UDP-glucose release, we examined the effect of the E-NPP inhibitor β,γ-metATP (Joseph *et al*., 2004) on the stability of UDP-[^{3}H]glucose, added as a radiotracer to 1321N1 cells. In the absence of β,γ-metATP, UDP-[^{3}H]glucose was gradually hydrolyzed with first-order rate constant (k) and half-life ($t_{1/2}$) values of 0.0329 min^{-1} and 21 min, respectively (Figure 1a). [^{3}H]Glucose-1P was the [^{3}H]-labelled product of UDP-[^{3}H]glucose hydrolysis on 1321N1 cells (data not shown), as previously described (Lazarowski *et al*., 2003b). β,γ-metATP effectively inhibited UDP-glucose hydrolysis. Figure 1a indicates that UDP-[^{3}H]glucose remained essentially unchanged on 1321N1 cells after 30 min in the presence of 300 μM β,γ-metATP. The concentration–effect relationship for β,γ-metATP inhibition of UDP-[^{3}H]glucose hydrolysis is illustrated

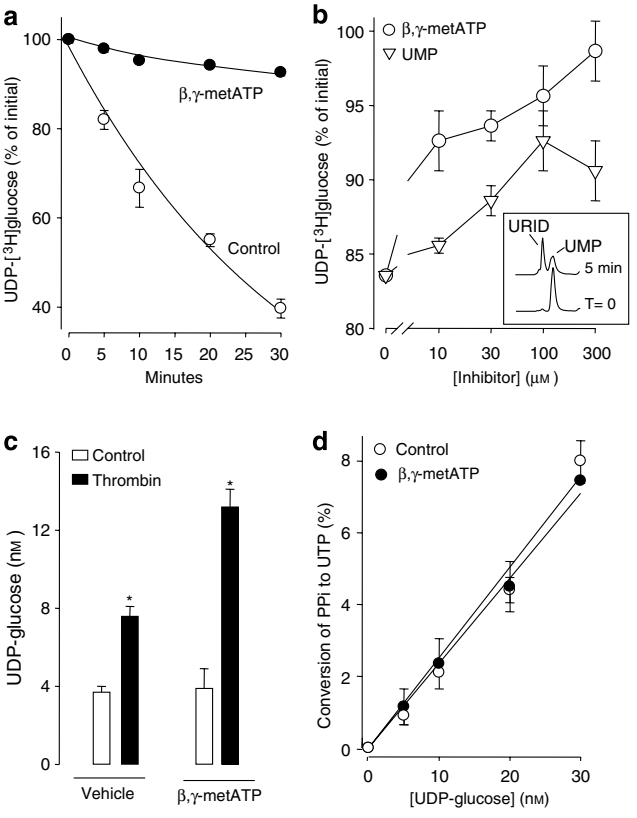

Figure 1 β,γ-methylene ATP is an effective inhibitor of hydrolysis of UDP-glucose. (**a**) Confluent 1321N1 cells were incubated in the absence (control) or presence of 300 μM β,γ-metATP and 0.1 μCi UDP-[^{3}H]glucose for the indicated times. Single exponential decay parameters k and $t_{1/2}$ were calculated as described previously (Lazarowski *et al*., 2000). (**b**) UDP-[^{3}H]glucose hydrolysis was assessed after a 5-min incubation with the indicated amount of β,γ-metATP or UMP; inset, HPLC tracing (absorbance at 260 nm) illustrating the conversion of UMP (100 μM) to uridine (URID) after 5 min. (**c**) Effect of β,γ-metATP (300 μM) on the release of UDP-glucose in response to 20 nM thrombin (5 min). (**d**) Calibration curve for the UDP-glucose assay in the absence or presence of 300 μM β,γ-metATP. The data represent the mean ± s.d. from at least two experiments performed in duplicate (**a**, **b** and **d**) or quadruplicate (**c**).

in Figure 1b. In the absence of an inhibitor, approximately 17% UDP-[^{3}H]glucose was hydrolyzed within 5 min (Figure 1b). Hydrolysis of UDP-[^{3}H]glucose was inhibited by approximately 50% with 10 μM β,γ-metATP, and was abolished with 300 μM β,γ-metATP (Figure 1b). UMP, the nucleotide product of E-NPP-catalyzed UDP-sugar hydrolysis, also inhibited UDP-[^{3}H]glucose breakdown, although less effectively than β,γ-metATP (Figure 1b). However, the magnitude of UMP inhibition on UDP-glucose hydrolysis could not be fully appreciated, because UMP itself was considerably hydrolyzed upon its addition to cells (Figure 1b, inset).

Previously, we reported that stimulation of 1321N1 with thrombin resulted in enhanced extracellular accumulation of UDP-glucose (Lazarowski, 2006), suggesting that thrombin promoted UDP-glucose release from these cells. To further corroborate this observation, extracellular UDP-glucose concentrations were measured in resting and thrombin-stimulated cells, in the absence or presence of β,γ-metATP. In resting, untreated cells, the concentration of UDP-glucose in the extracellular bulk medium was 3.7 ± 0.3 nM (Figure 1c). This UDP-glucose concentration reflected steady state where the rates of hydrolysis and constitutive release are equal (Lazarowski *et al*., 2000). Based on the *k* value obtained above (Figure 1a), the rate (*v*) of release of UDP-glucose from resting cells was calculated as $v = kS = 40\ \text{fmol min}^{-1}$, where *S* represents UDP-glucose concentration at steady state (Lazarowski *et al*., 2000, 2003b). Thus, in the absence of hydrolysis, that is, in the presence of β,γ-metATP, UDP-glucose concentrations in the 300 μl medium bathing a 12 mm culture would be predicted to increase at a pace of 0.09 nM min^{-1} (or 0.45 nM after 5 min), a minor increase. Indeed, average UDP-glucose concentration after the addition of β,γ-metATP to the cells for 5 min (3.9 ± 1.0 nM) was not significantly higher than control values (Figure 1c). However, levels of extracellular UDP-glucose increased to up to approximately 8 nM after the addition of 20 nM thrombin, and to approximately 14 nM when thrombin and β,γ-metATP were added in combination (Figure 1c). β,γ-metATP itself did not interfere with the measurement of UDP-glucose mass (Figure 1d). The most parsimonious explanation for the results in Figure 1 is that thrombin enhances the rate of release of UDP-glucose from 1321N1 cells. The data also suggest that, in the absence of inhibitors, E-NPP efficiently hydrolyses UDP-glucose at the site of release, as previously suggested for ATP (Joseph *et al*., 2003).

PAR1 promotes Ca^{2+}-dependent release of UDP-glucose and ATP

The time course for thrombin-elicited UDP-glucose release was examined in the presence of 300 μM β,γ-metATP. Addition of 20 nM thrombin to 1321N1 cells resulted in enhanced accumulation of extracellular UDP-glucose (3- to 4-fold increase within 1–5 min; Figure 2a). The PAR1-AP

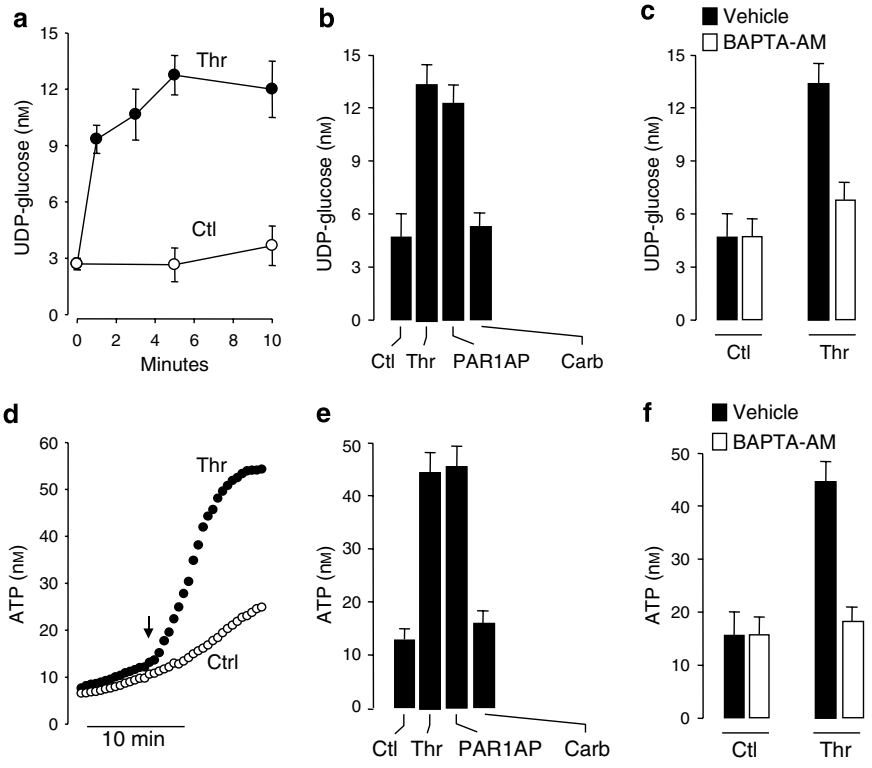

Figure 2 Agonist-promoted UDP-glucose and ATP release in 1321N1 cells. The cells were incubated with vehicle (Ctl) or 20 nM thrombin (Thr) for the indicated times (**a** and **d**), with vehicle, 20 nM thrombin, 100 μM PAR1-AP or 300 μM carbachol (Carb) for 5 min (**b** and **e**) or with vehicle or 20 nM thrombin for 5 min following a 30-min preincubation with 10 μM BAPTA-AM (**c** and **f**). UDP-glucose (**a**–**c**) and ATP (**d**–**f**) concentrations were measured as indicated in Methods. The data (in **a**–**c**, **e** and **f**) represent the mean ± s.d. of at least three experiments performed with quadruplicate samples. Representative tracings of ATP measurements in real time are illustrated in (**d**), and similar results were obtained in six independent experiments.

(100 μM; Figure 2b) caused a robust increase in UDP-glucose release, consistent with the notion that PAR1 is the major thrombin receptor expressed in 1321N1 cells (Majumdar *et al*., 1998). Reverse transcription-PCR analysis (and subsequent sequencing of products) verified that PAR1 transcripts were expressed in these cells (data not shown). As predicted from previous studies (Joseph *et al*., 2003), thrombin and PAR1-AP also caused enhanced ATP release from 1321N1 cells (Figures 2d and e). Changes in ATP concentration in response to thrombin were five times greater than that in UDP-glucose (Δ[ATP] ~50 nM, Δ[UDP-glucose] ~10 nM). However, whereas UDP-glucose was measured offline in diluted bulk medium, the ATP-sensing luciferin–luciferase protocol (Figures 2a–c) was optimized to assess ATP release near the cell surface (Okada *et al*., 2006). Both UDP-glucose and ATP release in response to thrombin were inhibited by incubating the cells with O,O′-Bis(2-aminophenyl)ethyleneglycol-*N*,*N*,*N*′,*N*′-teraacetic acid, tetraacetoxymethyl ester (BAPTA-AM) to chelate intracellular Ca^{2+} (Figures 2c and f). Unlike PAR1 agonists, the muscarinic receptor agonist carbachol (300 μM, 5 min) failed to elicit UDP-glucose and ATP release from 1321N1 cells (Figures 2b and e).

The above-mentioned results indicated that thrombin-elicited UDP-glucose and ATP release reflects a Ca^{2+}-dependent mechanism. However, the lack of effect of carbachol on nucleotide release was intriguing. We have previously shown a robust presence of G_q/PLC-β/Ca^{2+}-coupled muscarinic receptors in 1321N1 cells (Lazarowski *et al*., 1997). To investigate the possibility that differences in magnitude of G_q-mediated second messenger production between PAR-1 and muscarinic receptor activation accounted for differences in nucleotide release, concentration–response curves for agonist-promoted UDP-glucose release and inositol phosphate formation were generated. Thrombin promoted UDP-glucose release and inositol phosphate formation with EC_{50} values of 0.7 and 1.0 nM, respectively (Figure 3). PAR1-AP-elicited UDP-glucose release also occurred with a potency ($EC_{50} = 1.1$ μM) similar to that of PAR1-AP-promoted phosphoinositide breakdown ($EC_{50} = 0.7$ μM). At maximal concentrations, both thrombin and PAR1-AP increased UDP-glucose release and inositol phosphate formation by 7- to 9- and 4-folds, respectively (Figure 3). Carbachol promoted a robust (12-fold) increase in inositol lipid hydrolysis (Figure 3b) but elicited negligible UDP-glucose release at all concentrations tested (Figure 3a). These results suggest that receptor-promoted G_q/PLC-β activation is not sufficient to elicit nucleotide release from 1321N1 cells.

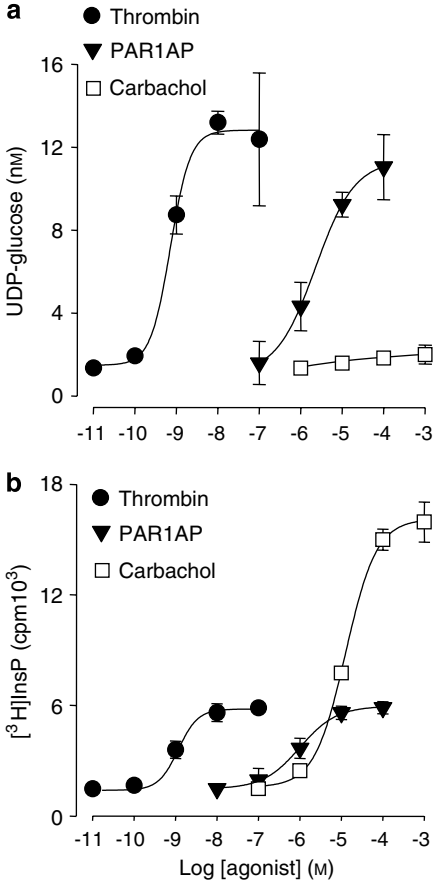

Figure 3 Concentration–response relationships for agonist-promoted UDP-glucose release and inositol phosphate formation in 1321N1 cells. (**a**) UDP-glucose release was measured following a 5-min incubation of cells in the presence of the indicated concentration of thrombin, PAR1-AP or carbachol. (**b**) *myo*-[^{3}H] inositol-labelled 1321N1 cells were incubated for 20 min in the presence of agonists, and the resulting [^{3}H]inositol phosphate accumulation quantified, as described in Methods. The results (mean ± s.d.) are from two (**a**) or three (**b**) independent experiments performed with triplicate samples.

UDP-glucose release is independent of G_i, PI3-kinase and Rho kinase

In addition to G_q, PAR1 couples to $G_{12/13}$ and G_i families of heterotrimeric G proteins (Majumdar *et al*., 1998; Ellis *et al*., 1999). In 1321N1 cells, PAR-promoted activation of $G_{12/13}$ leads to the activation of Rho GTPases. Among them, RhoA and its effector ROCK have been linked to actin cytoskeleton reorganization and changes in cell shape in 1321N1 cells (Majumdar *et al*., 1998). We investigated the effect of thrombin on cytoskeleton reorganization by confocal microscopy analysis of cells stained with fluorescently labelled phalloidin, which binds to F-actin. Resting 1321N1 cells displayed a fusiform and star-like shape (stellation), with long and thin cellular projections (usually contacting other cells) as well as short spine-like projections. The cells were flat and well attached to the substrate with actin stress fibres organized mainly along the longitudinal axes (Figure 4a). Incubation of 1321N1 cells with thrombin resulted in marked changes in cell shape and organization of the actin cytoskeleton. Most noticeable were the rounding and retraction of the cell body, loss of cell projections (reverse-stellation) and clustering of cells in bunches. Cell height increased notably, as indicated by *xz* laser-scanning analysis (data not shown). Intense actin-associated fluorescence was identified in the subplasma membrane compartment as a cortical ring (Figure 4a), as previously described (Coleman and Olson, 2002). Actin stress fibres decreased greatly. After 30 min of thrombin addition, many cells displayed blebbing-containing actin (Figures 4a, centre). In contrast to these effects of thrombin, no changes in cell shape/height were

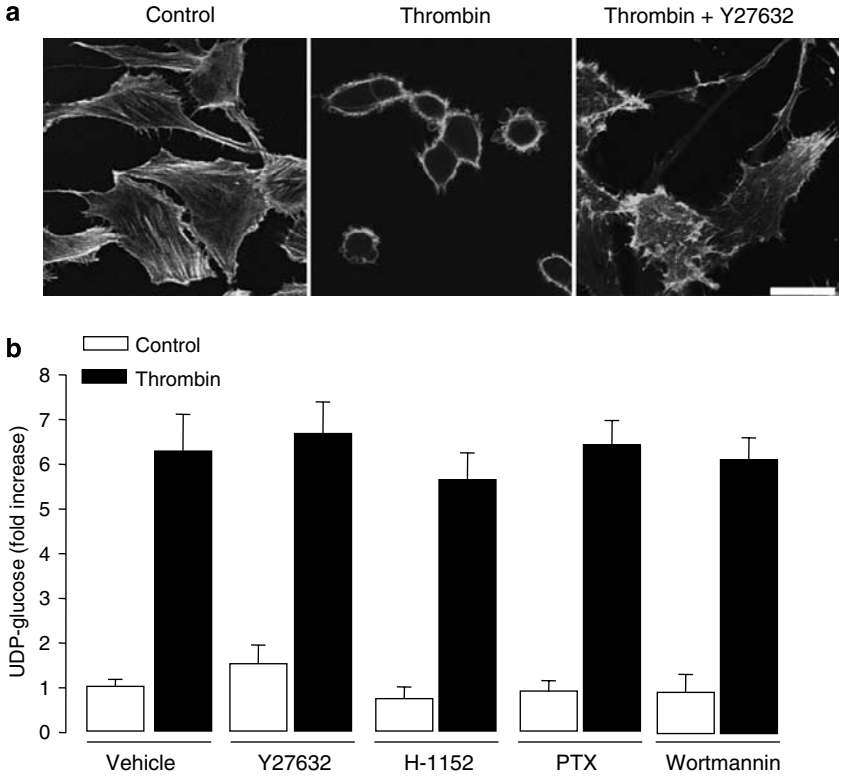

Figure 4 Lack of effect of Rho-kinase inhibitors, pertussis toxin and wortmannin on UDP-glucose release. (**a**) Y27632 inhibits thrombin-promoted cell rounding and actin cytoskeleton changes. 1321N1 cells were incubated for 30 min with vehicle or 20 nM thrombin in the absence or presence of 10 μM Y27632. Actin cytoskeleton was labelled with fluorescent phalloidin and visualized by confocal microscopy, as described in Methods; scale bar, 40 μm. (**b**) cells were preincubated in the presence of 10 μM Y27632 (30 min), 10 μM H-1152 (30 min), 100 nM wortmannin (15 min) or 60 ng ml^{-1} pertussis toxin (PTX, 18 h). The cells were subsequently incubated for an additional 10 min in the absence or presence of 20 nM thrombin. Extracellular UDP-glucose was measured as described in Methods. The results are expressed as fold increase relative to control (vehicle), and represent the mean ± s.d. from two independent experiments, each performed in quadruplicate.

observed in response to carbachol (data not shown). Preincubation of 1321N1 cells with the ROCK inhibitor Y27632 nearly abolished the effect of thrombin on cell rounding, reverse-stellation and cell blebbing (Figure 4a). These results are consistent with the notion that PAR1 activates $G_{12/13}$, which in turn promotes activation of the guanine nucleotide exchange factor (GEF) RhoGEF, upstream of Rho/ROCK (Trejo, 2003). However, Y27632, as well as H-1152, another selective ROCK inhibitor, failed to affect the magnitude of UDP-glucose release in thrombin-stimulated cells (Figure 4b).

Pertussis toxin, which ADP-ribosylates and inhibits $G\alpha_{i/o}$ proteins, also failed to affect thrombin-promoted UDP-glucose release. Consistent with these results, PI3-kinase (which is activated downstream of G_i) was not involved in UDP-glucose release, as judged by the absence of effect of wortmannin on thrombin-elicited UDP-glucose release (Figure 4b).

Exocytotic vs transport/conductive mechanisms

UDP-sugars are synthesized in the cytosol and transported to the lumen of the endoplasmic reticulum (ER) and the Golgi apparatus via UDP-sugar/UMP antiporters. These transporters translocate UDP-sugars from the cytosol to the lumen of the Golgi, using luminal UMP as the antiporter substrate (Hirschberg *et al*., 1998; Ishida and Kawakita, 2004). Although all known UDP-sugar transporters are ER/Golgi resident proteins, the possibility that an unknown UDP-glucose/UMP antiporter was expressed in the plasma membrane of 1321N1 cells, thereby exchanging cytosolic UDP-glucose for extracellular UMP, has not been formally examined. Preliminary experiments in our lab (performed in the absence of β,γ-metATP) suggested that UMP enhanced thrombin-promoted UDP-glucose release (data not shown). However, this effect was related to the inhibitory action of UMP on UDP-glucose hydrolysis (Figure 1b). As illustrated in Figure 5b, addition of exogenous UMP to the cells caused no changes in either basal or stimulated release of UDP-glucose (measured in the presence of β,γ-metATP). These results argue against the possibility that UDP-glucose release occurred via a plasma membrane UDP-sugar/UMP antiporter.

Alternatively, UDP-glucose release may reflect an exocytotic process (Lazarowski *et al*., 2003a). The fungal metabolite brefeldin A (BFA) disrupts retrograde movements along the secretory pathway, disassembling the Golgi network (Dinter and Berger, 1998; Shinotsuka *et al*., 2002). Incubation of 1321N1 cells with 3 μM BFA for 60 min provoked profound changes in Golgi morphology, as illustrated by the striking

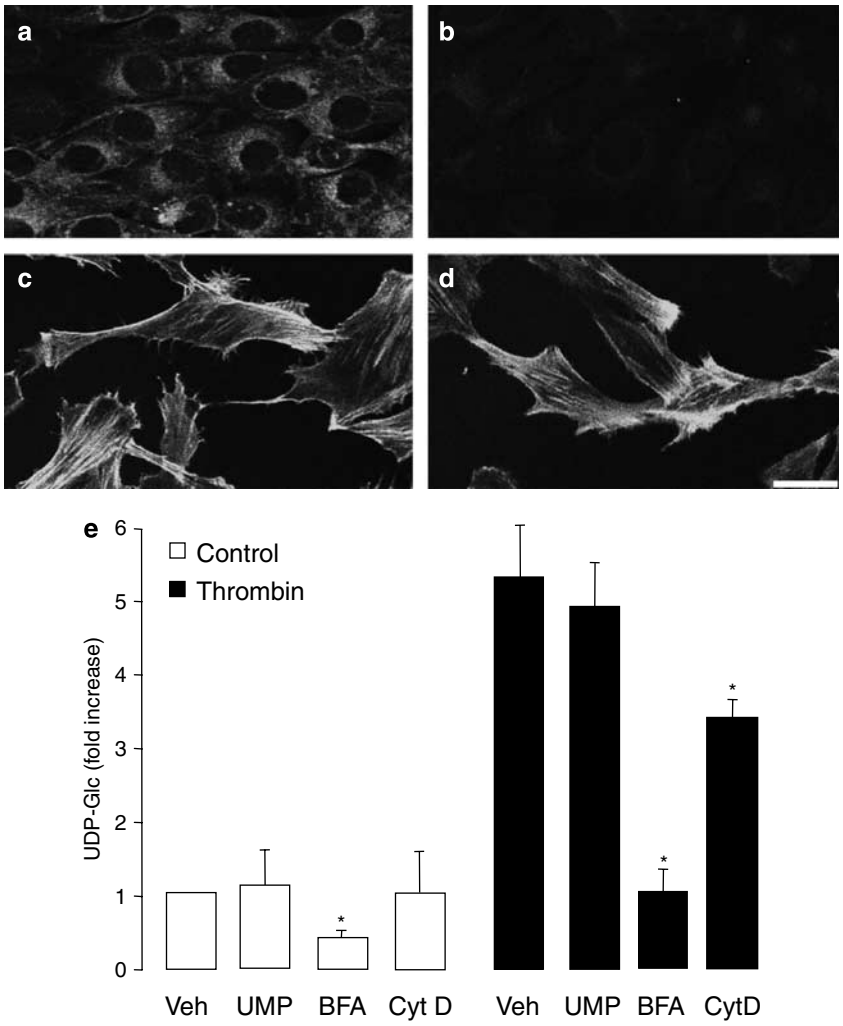

Figure 5 Inhibition of vesicle trafficking/exocytosis impairs receptor-promoted responses. (**a**–**d**) Brefeldin A (BFA) disrupted Golgi structures. 1321N1 cells were incubated for 1 h with vehicle (**a**, **c**) or 3 μM BFA (**b**, **d**). Golgi structures were labelled with NBD C_6-ceramide (**a**, **b**) and visualized by confocal microscopy. Actin cytoskeleton was labelled with fluorescent-phalloidin (**c**, **d**) to assess cell morphology; scale bar, 40 μm. (**e**) UDP-glucose measurements were performed in cells preincubated for 60 min in the presence of vehicle (Veh), 3 μM BFA or 10 μM cytochalasin D (CytD). At the end of this period, 300 μM β,γ-metATP was added to the cells. Cells were incubated for an additional 10 min in the absence or presence of 300 μM UMP and/or 20 nM thrombin, as indicated. The data represent the mean ± s.d. from at least two experiments performed in quadruplicates.

decrease in fluorescence attained with the Golgi marker NBD C_6-ceramide (Figures 5a and b). Treatment with BFA did not affect the overall cell morphology, as visualized by the actin fluorescent dye phalloidin (Figures 5c and d), and differential interface contrast images (data not shown). We have shown that BFA reduced basal UDP-glucose levels, consistent with the hypothesis that UDP-sugar release from resting cells is associated with the export of glycoconjugates to the cell surface, via the constitutive pathway (Lazarowski *et al*., 2003a). In our present experiments, BFA almost completely blocked thrombin (20 nM)-promoted UDP-glucose release (Figure 5e). Brefeldin A caused only partially inhibited thrombin-promoted [^{3}H]inositol phosphate formation (control, 4790 ± 360 cpm; BFA, 4610 ± 280 cpm; 20 nM thrombin, 12 770 ± 1680 cpm; thrombin plus BFA, 9050 ± 1187 cpm; $P<0.001$; $n=4$), which was consistent with the relatively rapid cell surface turnover of PAR1 (Trejo, 2003). BFA did not affect carbachol-elicited phosphoinositide breakdown (300 μM carbachol, 68 730 ± 9880 cpm; carbachol and BFA, 66 870 ± 2130 cpm; $n=4$), indicating that G_q-promoted signalling was preserved in BFA-treated cells. Thus, thrombin-evoked second messenger production, although diminished by BFA, was still robust. The partial (44%) reduction of PAR1-elicited signalling in the presence of BFA could not account for the dramatic reduction in PAR1-evoked UDP-glucose release observed under the same conditions. Furthermore, disruption of the cytoskeleton with cytochalasin D, a condition that inhibited vesicle exocytosis as well as ATP release in epithelial cells (Kreda *et al*., 2007), decreased (>30% inhibition) thrombin-elicited UDP-glucose release (Figure 5e) without affecting thrombin-evoked [^{3}H]inositol phosphate formation (data not shown). Altogether, the results in Figure 5 suggest that the secretory pathway was involved, at least in part, in both basal and in PAR-evoked UDP-glucose release from 1321N1 cells.

Discussion and conclusions

The major finding of the present study is that UDP-glucose release from 1321N1 astrocytes reflects a receptor-regulated, Ca^{2+}-dependent event, which requires the integrity of the secretory pathway. It was previously observed that 1321N1 cells release UDP-glucose constitutively (Lazarowski *et al*., 2003b), and that addition of thrombin to these cells resulted in increased accumulation of this nucleotide-sugar in the extracellular medium (Lazarowski, 2006). Our present work demonstrates that increased UDP-glucose accumulation in the medium of thrombin-stimulated cells reflected receptor-promoted release of this UDP-sugar rather than inhibition of nucleotide hydrolysis (Figure 1). We illustrated that thrombin promoted both UDP-glucose release and second messenger production with a potency consistent with this protease acting on PAR1 (Trejo, 2003). We also demonstrated that the PAR1-selective peptide TFLLRNPNDK elicited second messenger production and UDP-glucose release in 1321N1 cells with an efficacy similar to that of thrombin (Figure 3). Finally, Reverse transcription-PCR analysis confirmed expression of PAR1 transcripts in these cells. Our data strongly suggest that thrombin-promoted UDP-glucose release in 1321N1 cells was mediated by activation of PAR1.

Recently, we illustrated that elevation of Ca^{2+} (with ionomycin) was enough to induce nucleotide release from airway epithelial goblet cells, an event associated with Ca^{2+}-triggered exocytosis of mucin granules (Kreda *et al*., 2007). Consistent with the involvement of Ca^{2+} in nucleotide release, thrombin-evoked UDP-glucose release from 1321N1 cells was inhibited by BAPTA (added to cells as BAPTA-AM; Figure 2). However, a surprising finding of our current study was that agonist-promoted nucleotide release inversely correlated with the receptors' ability to evoke G_q/PLC signalling. The muscarinic M3 receptor is abundantly expressed on 1321N1 cells (Stephan and Sastry, 1992), and activation of these G_q-coupled/Ca^{2+}-mobilizing receptors did not result in UDP-glucose release. These results are in line with previous studies illustrating that carbachol evoked only minor ATP release from 1321N1 cells, relative to thrombin (Joseph *et al*., 2003). One possible explanation for our data is that UDP-glucose release in thrombin-stimulated 1321N1 cells reflected signalling downstream of PAR1/G_q that differed, spatially and/or temporally, from M3-receptor-evoked G_q signalling. Alternatively, as PAR1 couples to G_q, $G_{12/13}$ and G_i in 1321N1 cells, whereas muscarinic receptors on 1321N1 cells couple only to G_q (Majumdar *et al*., 1998), $G_{12/13}$ and/or G_i effectors may participate in thrombin-promoted nucleotide release from these cells. Our data do not support the involvement of G_i in PAR-stimulated UDP-glucose release. Pertussis toxin, which inhibits G_i signalling in 1321N1 cells (Parr *et al*., 1994), and wortmannin, an inhibitor of PI3-kinase (PI3-kinase-γ isoform is activated by G_i (Rickert *et al*., 2000)), had no effect on PAR1-stimulated UDP-glucose release (Figure 4b). It is well established that PAR1 coupling to $G_{12/13}$ leads to RhoGEF-mediated activation of Rho GTPases. A well-characterized downstream effector of Rho in 1321N1 cells is ROCK, which regulates morphologic changes. In 1321N1 cells, thrombin (but not carbachol) promotes myosin light change phosphorylation and cell shape changes, for example, cell rounding (Majumdar *et al*., 1998; Coleman and Olson, 2002). Although thrombin-elicited cell rounding was abolished in the presence of the ROCK inhibitor Y27632 (Figure 4a), thrombin-promoted UDP-glucose release was not affected by ROCK inhibitors (Figure 4b). Possibly, PAR-promoted nucleotide release could reflect involvement of effectors downstream of $G_{12/13}$ other than ROCK, for example, TKs, A-kinase anchoring protein, Ras GTPase activating protein, cadherin and PLC-ε (Kurose, 2003).

Apart from the signalling involved, regulated release of nucleotides is considered to occur in the following two possible modes: (i) cytosolic nucleotide release through channels or transporters and (ii) exocytotic release of nucleotide-enriched vesicles (Lazarowski *et al*., 2003a; Kreda *et al*., 2007). Candidate transporters mediating UDP-glucose release from the cytosol of 1321N1 cells are SLC35 translocators, which transport nucleotide-sugars across subcellular membranes (Hirschberg *et al*., 1998; Ishida and Kawakita, 2004). SLC35 translocators transport UDP-glucose and other UDP-sugars from the cytosol to the ER/Golgi, using luminal UMP as the antiporter substrate (Hirschberg *et al*., 1998; Ishida and Kawakita, 2004). However, UDP-sugar/UMP translocators does not appear to be expressed/inserted in the plasma membrane of 1321N1 cells, as addition of UMP to the extracellular medium failed to increase UDP-glucose release (Figure 5). Moreover, the robust ecto-5′-nucleotidase activity present on 1321N1 cells (Figure 1b) makes it unlikely that endogenous UMP (for example, generated from released UTP; Lazarowski *et al*., 1997) accumulates on 1321N1 cell surfaces. Furthermore, the fact that UDP-glucose release from thrombin-stimulated 1321N1 cells was accompanied by enhanced ATP release suggests that a non-selective mechanism was involved. We cannot rule out that channels or transporters, other than SLC35, facilitated cytosolic nucleotide release from 1321N1 cells. For example, connexin and pannexin hemichannels have been proposed as ATP channels in several types of cells (Cotrina *et al*., 1998; Stout *et al*., 2002; Bao *et al*., 2004; De Vuyst *et al*., 2005; Eltzschig *et al*., 2006; Pelegrin and Surprenant, 2006; Huang *et al*., 2007). The potential contribution of connexin hemichannels to nucleotide release from astrocytes is unclear (Scemes *et al*., 2000; Coco *et al*., 2003; Bowser and Khakh, 2007).

Neurons, chromaffin cells, platelets, mast cells and pancreatic acinar cells package ATP in synaptic vesicles, chromaffin granules or dense core granules, which, upon stimulation with, for instance Ca^{2+} mobilizing agonists, fuse with the plasma membrane and release their contents into the extracellular space, a process commonly referred to as regulated exocytosis (Dean *et al*., 1984; Evans *et al*., 1992; Gualix *et al*., 1999; Sorensen and Novak, 2001). Coco *et al*. (2003) have illustrated that an ATP-rich fraction from astrocyte homogenates co-sedimented with secretogranin II-containing vesicles on sucrose density gradients, and that mechanically induced ATP release was Ca^{2+}-dependent and was inhibited by tetanus neurotoxin and the v-ATPase inhibitor bafilomycin A_1. These findings support the hypothesis that ATP release in mechanically stimulated astrocytes occur via regulated exocytosis (Coco *et al*., 2003). Our observation that UDP-glucose is released concomitantly with

ATP from PAR-stimulated 1321N1 astrocytoma cells supports the involvement of vesicles in nucleotide release from astrocytes. UDP-glucose is utilized in the lumen of the ER and Golgi for quality control of glycoproteins. UDP-glucose is the glucose donor substrate for glucosylation of denatured domains of newly synthesized glycoproteins (Hirschberg *et al*., 1998). Like UDP-sugars, ATP is also transported to and used as an energy source within the ER/Golgi (Hirschberg *et al*., 1998). Nucleotides imported to the lumen of the ER and Golgi reach concentrations up to 20-fold higher than their cytosolic levels, and are not transported back to the cytosol (Hirschberg *et al*., 1998). Therefore, they are likely to be delivered as cargo molecules and released from cells during glycoprotein secretion. Our data illustrating that UDP-glucose release was inhibited by BFA (Figure 5b) further suggest (although do not prove) that nucleotides were released from the secretory pathway.

However, the hypothesis that nucleotide release is associated with agonist-promoted vesicle exocytosis has been difficult to test in 1321N1 cells, using styryl fluorophores, for example, FM 1-43 (Kreda *et al*., 2007; Tatur *et al*., 2008). Unlike most cells, 1321N1 cells displayed a steady, robust increase of FM 1-43- (or its analogues FM 2-10 or FM 1-64) associated fluorescence in the absence of stimuli, which precluded using these protocols to assess thrombin-promoted exocytosis in these cells (Kreda SM, unpublished data). Lowering the temperature has been used to assess the contribution of exocytosis to nucleotide release in several cell types. However, incubating 1321N1 cells at 16 °C markedly inhibited agonist-promoted [^{3}H]inositol phosphate formation (>95% inhibition, data not shown), discouraging us from assessing the effect of temperature changes on agonist-evoked UDP-glucose release.

Regardless of the cellular pathways and mechanism(s) regulating UDP-glucose release from astrocytes, an understanding of the physiological processes regulated by the UDP-glucose-sensing $P2Y_{14}$ receptor in glial cells and astrocytes is now emerging (Fumagalli *et al*., 2003; Lee *et al*., 2003; Moore *et al*., 2003; Skelton *et al*., 2003; Bianco *et al*., 2005; Abbracchio and Verderio, 2006; Kobayashi *et al*., 2006). $P2Y_{14}$ receptor transcripts (Chambers *et al*., 2000), as well as $P2Y_{14}$ receptor-associated immunoreactivity (Moore *et al*., 2003), are abundantly detected through several regions of the brain. Immunohistochemistry analysis of post-mortem human brain suggests that $P2Y_{14}$ receptor localizes specifically to astrocytes. Functional evidence of $P2Y_{14}$ receptor expression in astrocytes has been suggested by studies illustrating UDP-glucose-promoted Ca^{2+} mobilization in primary cultures of rat glial cells and cortical astrocytes (Fumagalli *et al*., 2003; Bianco *et al*., 2005). Expression of $P2Y_{14}$ receptor mRNA in the rat brain is upregulated by immunological challenge (Moore *et al*., 2003; Bianco *et al*., 2005), suggesting that the receptor is involved in reactive astrogliosis.

PAR-activated astrocytes (Wang and Reiser, 2003) may be an additional source of regulated release of UDP-glucose. The interstitial fluid volume in the brain has been estimated to be approximately 200 μl g^{-1} (Friden *et al*., 2007). As there are 1–5 trillion cells in the adult human brain (~1.4 kg weight), a conservative estimation of the volume of the interstitial fluid surrounding the cells would yield 200 nl per 10^6 cells. UDP-glucose released to the bulk medium following thrombin stimulation represented approximately 3 pmol per 10^6 cells (Figure 2). Therefore, on the basis of these assumptions, UDP-glucose concentration in the undiluted extracellular milieu of PAR-stimulated astrocytes could approach a value of 10–20 μM, which is in the range for promoting robust $P2Y_{14}$ receptor activation (Chambers *et al*., 2000; Lazarowski *et al*., 2003b).

In summary, our study illustrates, for the first time, the occurrence of Ca^{2+}-dependent release of UDP-glucose in receptor-stimulated 1321N1 astrocytes. Thus, UDP-glucose release reflects a physiologically regulated mechanism of nucleotide release, as opposed to nucleotide leakage from damaged cells. Demonstration of the regulated release of UDP-glucose, the most potent and selective naturally occurring $P2Y_{14}$ receptor agonist, provides compelling evidence that, in addition to its well-established role in metabolic reactions, this nucleotide-sugar plays important roles in intercellular signalling.

Acknowledgements

We thank Dr Wanda O'Neal and Lisa Jones for technical assistance for PCR protocols and sequencing analysis, Dr JoAnn Trejo for kindly providing PAR1 primers, Drs Richard C Boucher and T Ken Harden for helpful discussions and comments and Lisa Brown for editorial assistance. We also thank the UNC Michael Hooker Microscopy Facility for the use of microscopes. This work was supported by NIH P01-HL034322.

Conflict of interest

The authors state no conflict of interest.

References

Abbracchio MP, Verderio C (2006). Pathophysiological roles of P2 receptors in glial cells. *Novartis Found Symp* **276**: 91–103.

Bao L, Locovei S, Dahl G (2004). Pannexin membrane channels are mechanosensitive conduits for ATP. *FEBS Lett* **572**: 65–68.

Bianco F, Fumagalli M, Pravettoni E, D'Ambrosi N, Volonte C, Matteoli M *et al.* (2005). Pathophysiological roles of extracellular nucleotides in glial cells: differential expression of purinergic receptors in resting and activated microglia. *Brain Res Brain Res Rev* **48**: 144–156.

Bowser DN, Khakh BS (2007). Vesicular ATP is the predominant cause of intercellular calcium waves in astrocytes. *J Gen Physiol* **129**: 485–491.

Burnstock G (2006). Purinergic signalling. *Br J Pharmacol* **147** (Suppl 1): S172–S181.

Burnstock G, Williams M (2000). P2 purinergic receptors: modulation of cell function and therapeutic potential. *J Pharmacol Exp Ther* **295**: 862–869.

Chambers JK, Macdonald LE, Sarau HM, Ames RS, Freeman K, Foley JJ *et al.* (2000). A G protein-coupled receptor for UDP-glucose. *J Biol Chem* **275**: 10767–10771.

Coco S, Calegari F, Pravettoni E, Pozzi D, Taverna E, Rosa P *et al.* (2003). Storage and release of ATP from astrocytes in culture. *J Biol Chem* **278**: 1354–1362.

Coleman ML, Olson MF (2002). Rho GTPase signalling pathways in the morphological changes associated with apoptosis. *Cell Death Differ* **9**: 493–504.

Cotrina ML, Lin JH, Alves-Rodrigues A, Liu S, Li J, Azmi-Ghadimi H *et al.* (1998). Connexins regulate calcium signaling by controlling ATP release. *Proc Natl Acad Sci USA* **95**: 15735–15740.

Damiano BP, Cheung WM, Santulli RJ, Fung-Leung WP, Ngo K, Ye RD *et al.* (1999). Cardiovascular responses mediated by protease-activated receptor-2 (PAR-2) and thrombin receptor (PAR-1) are distinguished in mice deficient in PAR-2 or PAR-1. *J Pharmacol Exp Ther* **288**: 671–678.

De Vuyst E, Decrock E, Cabooter L, Dubyak GR, Naus CC, Evans WH *et al.* (2005). Intracellular calcium changes trigger connexin 32 hemichannel opening. *EMBO J* **25**: 34–44.

Dean GE, Fishkes H, Nelson PJ, Rudnick G (1984). The hydrogen ion-pumping adenosine triphosphatase of platelet dense granule membrane. Differences from F1F0- and phosphoenzyme-type ATPases. *J Biol Chem* **259**: 9569–9574.

Dinter A, Berger EG (1998). Golgi-disturbing agents. *Histochem Cell Biol* **109**: 571–590.

Ellis CA, Malik AB, Gilchrist A, Hamm H, Sandoval R, Voyno-Yasenetskaya T *et al.* (1999). Thrombin induces proteinase-activated receptor-1 gene expression in endothelial cells via activation of G_i-linked Ras/mitogen-activated protein kinase pathway. *J Biol Chem* **274**: 13718–13727.

Eltzschig HK, Eckle T, Mager A, Kuper N, Karcher C, Weissmuller T *et al.* (2006). ATP release from activated neutrophils occurs via connexin 43 and modulates adenosine-dependent endothelial cell function. *Circ Res* **99**: 1100–1108.

Evans RJ, Derkach V, Surprenant A (1992). ATP mediates fast synaptic transmission in mammalian neurons. *Nature* **357**: 503–505.

Friden M, Gupta A, Antonsson M, Bredberg U, Hammarlund-Udenaes M (2007). *In vitro* methods for estimating unbound drug concentrations in the brain interstitial and intracellular fluids. *Drug Metab Dispos* **35**: 1711–1719.

Fumagalli M, Brambilla R, D'Ambrosi N, Volonte C, Matteoli M, Verderio C *et al.* (2003). Nucleotide-mediated calcium signaling in rat cortical astrocytes: role of P2X and P2Y receptors. *Glia* **43**: 218–230.

Gualix J, Pintor J, Miras-Portugal MT (1999). Characterization of nucleotide transport into rat brain synaptic vesicles. *J Neurochem* **73**: 1098–1104.

Hirschberg CB, Robbins PW, Abeijon C (1998). Transporters of nucleotide sugars, ATP, and nucleotide sulfate in the endoplasmic reticulum and Golgi apparatus. *Annu Rev Biochem* **67**: 49–69.

Huang YJ, Maruyama Y, Dvoryanchikov G, Pereira E, Chaudhari N, Roper SD (2007). The role of pannexin 1 hemichannels in ATP release and cell–cell communication in mouse taste buds. *Proc Natl Acad Sci USA* **104**: 6436–6441.

Ishida N, Kawakita M (2004). Molecular physiology and pathology of the nucleotide sugar transporter family (SLC35). *Pflugers Arch* **447**: 768–775.

Joseph SM, Buchakjian MR, Dubyak GR (2003). Colocalization of ATP release sites and ecto-ATPase activity at the extracellular surface of human astrocytes. *J Biol Chem* **278**: 23342.

Joseph SM, Pifer MA, Przybylski RJ, Dubyak GR (2004). Methylene ATP analogs as modulators of extracellular ATP metabolism and accumulation. *Br J Pharmacol* **142**: 1002–1014.

Kobayashi K, Fukuoka T, Yamanaka H, Dai Y, Obata K, Tokunaga A *et al.* (2006). Neurons and glial cells differentially express P2Y receptor mRNAs in the rat dorsal root ganglion and spinal cord. *J Comp Neurol* **498**: 443–454.

Kreda SM, Okada SF, van Heusden CA, O'Neal W, Gabriel S, Abdullah L *et al.* (2007). Coordinated release of nucleotides and mucin from human airway epithelial Calu-3 cells. *J Physiol* **584**: 245–259.

Kurose H (2003). Galpha12 and Galpha13 as key regulatory mediator in signal transduction. *Life Sci* **74**: 155–161.

Lazarowski E (2006). Regulated release of nucleotides and UDP-sugars from astrocytoma cells. In: Chadwick DJ, Goode J (eds). *Purinergic Signaling in Neuron–Glia Interactions*. Wiley: London. pp 73–90.

Lazarowski ER, Boucher RC, Harden TK (2000). Constitutive release of ATP and evidence for major contribution of ecto-nucleotide pyrophosphatase and nucleoside diphosphokinase to extracellular nucleotide concentrations. *J Biol Chem* **275**: 31061–31068.

Lazarowski ER, Boucher RC, Harden TK (2003a). Mechanisms of release of nucleotides and integration of their action as P2X- and P2Y-receptor activating molecules. *Mol Pharmacol* **64**: 785–795.

Lazarowski ER, Homolya L, Boucher RC, Harden TK (1997). Direct demonstration of mechanically induced release of cellular UTP and its implication for uridine nucleotide receptor activation. *J Biol Chem* **272**: 24348–24354.

Lazarowski ER, Shea DA, Boucher RC, Harden TK (2003b). Release of cellular UDP-glucose as a potential extracellular signaling molecule. *Mol Pharmacol* **63**: 1190–1197.

Lazarowski ER, Tarran R, Grubb BR, van Heusden CA, Okada S, Boucher RC (2004). Nucleotide release provides a mechanism for airway surface liquid homeostasis. *J Biol Chem* **279**: 36855–36864.

Lee BC, Cheng T, Adams GB, Attar EC, Miura N, Lee SB *et al.* (2003). P2Y-like receptor, GPR105 (P2Y14), identifies and mediates chemotaxis of bone-marrow hematopoietic stem cells. *Genes Dev* **17**: 1592–1604.

Majumdar M, Seasholtz TM, Goldstein D, de Lanerolle P, Brown JH (1998). Requirement for Rho-mediated myosin light chain phosphorylation in thrombin-stimulated cell rounding and its dissociation from mitogenesis. *J Biol Chem* **273**: 10099–10106.

Moore DJ, Murdock PR, Watson JM, Faull RL, Waldvogel HJ, Szekeres PG *et al.* (2003). GPR105, a novel $G_{i/o}$-coupled UDP-glucose receptor expressed on brain glia and peripheral immune cells, is regulated by immunologic challenge: possible role in neuroimmune function. *Brain Res Mol Brain Res* **118**: 10–23.

Okada SF, Nicholas RA, Kreda SM, Lazarowski ER, Boucher RC (2006). Physiological regulation of ATP release at the apical surface of human airway epithelia. *J Biol Chem* **281**: 22992–23002.

Parr CE, Sullivan DM, Paradiso AM, Lazarowski ER, Burch LH, Olsen JC *et al.* (1994). Cloning and expression of a human-P(2U) nucleotide receptor, a target for cystic-fibrosis pharmacotherapy. *Proc Natl Acad Sci USA* **91**: 3275–3279.

Pelegrin P, Surprenant A (2006). Pannexin-1 mediates large pore formation and interleukin-1beta release by the ATP-gated P2X7 receptor. *EMBO J* **25**: 5071–5082.

Rickert P, Weiner OD, Wang F, Bourne HR, Servant G (2000). Leukocytes navigate by compass: roles of PI3Kgamma and its lipid products. *Trends Cell Biol* **10**: 466–473.

Scemes E, Suadicani SO, Spray DC (2000). Intercellular communication in spinal cord astrocytes: fine tuning between gap junctions and P2 nucleotide receptors in calcium wave propagation. *J Neurosci* **20**: 1435–1445.

Shinotsuka C, Yoshida Y, Kawamoto K, Takatsu H, Nakayama K (2002). Overexpression of an ADP-ribosylation factor-guanine nucleotide exchange factor, BIG2, uncouples brefeldin A-induced adaptor protein-1 coat dissociation and membrane tubulation. *J Biol Chem* **277**: 9468–9473.

Skelton L, Cooper M, Murphy M, Platt A (2003). Human immature monocyte-derived dendritic cells express the G protein-coupled receptor GPR105 (KIAA0001, P2Y14) and increase intracellular calcium in response to its agonist, uridine diphosphoglucose. *J Immunol* **171**: 1941–1949.

Sorensen CE, Novak I (2001). Visualization of ATP release in pancreatic acini in response to cholinergic stimulus. Use of fluorescent probes and confocal microscopy. *J Biol Chem* **276**: 32925–32932.

Stephan CC, Sastry BV (1992). Characterization of the subtype of muscarinic receptor coupled to the stimulation of phosphoinositide hydrolysis in 132-1N1 human astrocytoma cells. *Cell Mol Biol (Noisy-le-grand)* **38**: 701–712.

Stout CE, Costantin JL, Naus CC, Charles AC (2002). Intercellular calcium signaling in astrocytes via ATP release through connexin hemichannels. *J Biol Chem* **277**: 10482–10488.

Tatur SS, Kreda S, Lazarowski ER, Grygorczyk R (2008). Calcium-dependent release of adenine and uridine nucleotides from A549 cells. *Purinergic Signal*, http://www.springer.com/west/home/biomed?SGWID=4-124-70-34307308-0&detailsPage=journal%7CaimsAndScopes.

Trejo J (2003). Protease-activated receptors: new concepts in regulation of G protein-coupled receptor signaling and trafficking. *J Pharmacol Exp Ther* **307**: 437–442.

Wang H, Reiser G (2003). Thrombin signaling in the brain: the role of protease-activated receptors. *Biol Chem* **384**: 193–202.